

The Early Bird Catches the Leak: Unveiling Timing Side Channels in LLM Serving Systems^{*}

Linke Song^{*§}, Zixuan Pang[†], Wenhao Wang^{*§✉}, Zihao Wang[‡], XiaoFeng Wang[‡],
Hongbo Chen[‡], Wei Song^{*§}, Yier Jin[†], Dan Meng^{*}, Rui Hou^{*}

^{*}*Institute of Information Engineering, CAS* [†]*University of Science and Technology of China*
[‡]*Indiana University Bloomington*
[§]*School of Cyber Security, University of Chinese Academy of Sciences*

Abstract

The wide deployment of Large Language Models (LLMs) has given rise to strong demands for optimizing their inference performance. Today's techniques serving this purpose primarily focus on reducing latency and improving throughput through algorithmic and hardware enhancements, while largely overlooking their privacy side effects, particularly in a multi-user environment. In our research, for the first time, we discovered a set of new timing side channels in LLM systems, arising from shared caches and GPU memory allocations, which can be exploited to infer both confidential system prompts and those issued by other users. These vulnerabilities echo security challenges observed in traditional computing systems, highlighting an urgent need to address potential information leakage in LLM serving infrastructures.

In this paper, we report novel attack strategies designed to exploit such timing side channels inherent in LLM deployments, specifically targeting the Key-Value (KV) cache and semantic cache widely used to enhance LLM inference performance. Our approach leverages timing measurements and classification models to detect cache hits, allowing an adversary to infer private prompts with high accuracy. We also propose a token-by-token search algorithm to efficiently recover shared prompt prefixes in the caches, showing the feasibility of stealing system prompts and those produced by peer users. Our experimental studies on black-box testing of popular online LLM services demonstrate that such privacy risks are completely realistic, with significant consequences. Our findings underscore the need for robust mitigation to protect LLM systems against such emerging threats.

1 Introduction

Large Language Models (LLMs) are widely used in applications like chatbots [14, 20], search engines [35], and

coding assistants [23]. However, LLM inference is resource-intensive, demanding substantial computational power and memory due to the model's vast parameters, numerous layers, and large context sizes. Improving LLM inference performance has thus become crucial, prompting solutions such as weight quantization [49, 61, 78, 80, 84], model compression [66, 76, 94], algorithm optimization [45, 58, 81], hardware improvements [73, 90], and parallel processing techniques [86]. These approaches aim to reduce latency and enhance inference performance [64], though their privacy implications remain less clear.

In this paper, we present the first security analysis of performance optimization techniques used by modern LLM systems that serve multiple users or applications simultaneously. Our research uncovers significant information leaks from unique side channels introduced by these techniques. Specifically, existing LLM performance optimizations employ shared caches to reduce computation and storage overhead during inference. However, memory sharing, cache contention and eviction, and GPU scheduling among different users and applications can interfere with user requests, creating observable timing side channels. Exploiting these side channels can reveal private prompts from other users or applications.

LLM cache channels. In our research, we focused on various caches in LLM systems, which not only reduce the computation cost of LLM inference but also enhance user experience by lowering service latency. We found that these caches can be exploited to infer proprietary system prompts or sensitive prompts from peer users. These prompts not only contain private user information but also hold commercial value, as they enable an LLM to perform various downstream tasks efficiently without fine-tuning. We identified the following two cache channels:

- *Leakage from sharing the KV cache.* Efficient inference requires careful allocation of GPU memory. For each inference request, an LLM maintains an in-memory state called the KV cache, which is reused in every iteration throughout the entire process of serving the request and generating

^{*}The two lead authors contribute equally to the work. Corresponding author: Wenhao Wang (wangwenhao@iie.ac.cn).

the response. Due to the causal attention mask in LLMs, each token’s activations are influenced only by preceding tokens in the sequence. Therefore, if multiple requests share a common prefix, the keys and values corresponding to the prefix tokens are identical across sequences. To optimize memory usage of the KV cache, the system can identify matching prompt prefixes across multiple requests and share their key/value tensors in memory at runtime [58, 91]. This sharing occurs when prompts have a common prefix, which often happens with few-shot examples [70], chatbot system prompts [51], or prompt templates [37]. For instance, it has been reported that Claude’s prompt caching feature can reduce costs by up to 90% and decrease latency by up to 85% for long prompts [36].

- *Leakage from sharing the semantic cache.* The semantic cache [44] enhances the performance of LLM applications by caching responses based on the semantic meaning or context of the queries. For instance, for the queries "give me suggestions for a comedy movie" and "recommend a comedy movie," the LLM system detects their semantic similarity and returns similar responses without querying the LLM. It has been shown that when GPTCache is integrated with OpenAI’s GPT service, response speed can be increased by a factor of 2 to 10 when the cache is hit [44].

Challenges and solutions. A straightforward way to exploit these vulnerable caches is to directly search the prompt space for one that causes a cache hit. However, this approach is ineffective for several reasons. Firstly, the timing difference from hitting a single cache block is usually minimal and can easily blend with natural variations in network latency, making it difficult to detect and exploit. Additionally, since the KV cache can only be reused when prompts share a common prefix, this further limits attack opportunities. Secondly, the prompt search space is large, making it challenging to systematically explore all possible prompts to find the cached one. Moreover, during this process, the attacker’s own requests may also be cached, adding noise to subsequent requests and potentially causing the victim’s requests to be evicted.

To address these challenges, we designed several attack strategies to exploit LLM side channels. Specifically, we used a classification model to detect token-level KV cache hits based on timing measurements in an offline phase. By adjusting the timing threshold, we found that online detection accuracy can be significantly improved with only a few repetitive trials. To reduce the search space, we proposed an incremental search algorithm for the KV cache channel, leveraging the fact that the KV cache can only be reused if requests share a common prefix. This allows recovery of the prompt token on a per-token basis. For the semantic cache channel, we developed an algorithm to identify the most representative prompts for given semantics as the attacker’s requests. To minimize noise introduced by attack requests, we utilized the caching system’s support to efficiently flush the KV cache. For the

semantic cache, our attack ensures that the trials performed by the attacker do not overlap by computing their semantic similarities.

Experimental studies. In our research, we verified the presence of vulnerabilities in open-source projects, including SGLang [40], Langchain [27], and GPTCache [24] in our local environment. Building on these findings, we demonstrate the potential to deduce proprietary system prompts (i.e., *prompt stealing attack*) or infer sensitive requests from neighboring users (i.e., *peeping neighbor attack*).

For the prompt stealing attack, our evaluation shows that the accuracy of detecting a per-token hit or miss in the KV cache is 86%, with a false positive rate (FPR) of 5% using 100 LLM queries. With the incremental search algorithm, we effectively recovered the system prompt token by token, with each token requiring an average of 234 queries, resulting in an average recovery accuracy of 92.3%. For the peeping neighbor attack, the accuracy of identifying cache hits and misses is 85.3%, with an FPR of 3.2% in a single trial, and over 95% accuracy with an FPR of 3.6% after three trials under GPTCache’s default parameters.

Furthermore, we found that common LLM deployment practices, such as Retrieval-Augmented Generation (RAG), introduce timing vulnerabilities that can be exploited to infer documents and websites processed by the LLM. Our black-box measurement study of existing online services reveals that popular LLM systems, such as OpenAI’s GPT-4 and Google’s Gemini, use KV or semantic cache sharing to reduce costs, making them vulnerable to timing side-channel attacks.

Finally, we developed preliminary defenses against the side-channel risks identified. To mitigate KV cache leakage, we propose that prefix caches should only be shared in units of at least k tokens ($k = 2, 3, 4$, etc.). As the search space increases with k , the attack requires more guesses and additional queries, but the timing difference for sharing a larger number of tokens also increases, enabling more robust classifiers. Thus, the attack remains highly accurate, albeit with increased LLM queries. To reduce semantic cache leakage, we recommend identifying and anonymizing privacy-related information within user inputs before conducting a search for semantic similarity. Initial evaluations indicate that this mitigation incurs a marginal overhead (approximately 4%).

Contributions. Our paper makes the following contributions:

- *New discovery.* We discovered new timing side channels in both open-source and online LLM serving systems, arising from the sharing of the semantic cache and KV cache to reduce inference costs.
- *Novel exploit strategies.* We proposed new attack strategies to exploit the side channels inherent in LLM inference optimization, which enables two novel attacks: prompt stealing attack and peeping neighbour attack.
- *Experimental validations, real-world measurements and mitigation.* We verified side-channel leakages in prominent

LLM systems locally and conducted a black-box study of popular online LLM services, providing preliminary solutions to mitigate these risks.

2 Background

2.1 LLM Serving Systems

In this paper, we explore the deployment of a shared LLM to cater to multiple users or applications within a computing system. This scenario is commonly encountered in public services provided by commercial companies, such as the OpenAI chatbot. This concept is also applicable to locally-deployed shared LLM models that serve multiple applications. Specifically, the rise of LLMs has enabled LLM-based applications (a.k.a. AI agents or co-pilots), a new software paradigm that combines the strength of LLM and conventional software. With the emergence of LLM as an operating system (e.g., AIOS [63]) and agents as Apps, multiple LLM applications or agents can operate on the same LLM, acting as a shared foundational model. These LLM agents are usually developed and utilized by different developers and applications. Additionally, this concept extends to local LLM within a browser environment. For example, Lumos [31] is a Chrome extension powered by Ollama, a RAG LLM co-pilot designed for web browsing, utilizing local LLMs for inference without the need for remote server support.

In the aforementioned scenarios, the LLM is typically optimized to achieve optimal latency and throughput by focusing on memory usage optimization, efficient batching, and effective scheduling decisions. However, challenges arise due to memory sharing, cache contentions and evictions, and GPU scheduling among different users and applications. These factors can introduce interference among multiple requests, potentially creating observable timing side channels. As these users and applications are not mutually trusted, there is a risk of sensitive information leakage. This includes the possibility of divulging other users' or applications' secrets, such as sensitive request input, proprietary system prompts, or prompt templates, through timing side channels.

2.2 Serving Frontend

LLM serving modes. The LLM service provides two operation modes. In non-streaming mode, the response is computed and delivered as a complete response after processing the request. However, when generating long completions, this method can lead to a substantial waiting time of several seconds. To receive faster responses, the streaming mode is available. In this mode, the LLM tokens are emitted sequentially, allowing users to see the initial part of the completion before the entire response is fully generated. Streaming is the preferred way to interact with LLMs, particularly in scenarios like chatbot, where real-time conversations are essential.

Popular LLM applications (e.g., Bing Copilot [12], ChatGPT [14]) use a system prompt containing task definitions, examples, and safety rules to guide their behavior. This prompt is typically static and shared among all users.

Metrics. Latency is a crucial metric that measures the time it takes for an LLM to generate a response to a user's prompt. It plays a significant role in shaping the user's perception of the speed and efficiency of a generative AI application. Low latency is particularly important in use cases involving real-time interactions, such as chatbot and AI copilots.

Time To First Token (TTFT) measures the duration between the user entering a prompt and receiving the first token of the model's response. It reflects the time required to process the user's input and generate the initial completion token. On the other hand, total generation time refers to the end-to-end latency of an LLM, encompassing the entire process from the user entering the prompt to receiving the completed output from the model.

Throughput, on the other hand, quantifies the capacity of an LLM to process requests or generate output within a specific time frame. Requests per second is influenced by the total generation time of the model, which itself depends on the length of the model's output. Therefore, tokens per second is a more commonly used metric for measuring throughput.

2.3 Serving Backend

LLM inference consists of two stages: a prefill phase and a decoding phase. The prefill phase processes the entire input prompt and produces the first output token, while the decoding phase generates the rest of output tokens, one-at-a-time.

Prefill phase. In the prefill phase, the LLM engine takes the request prompt as input and converts it into a series of input tokens. A token is a unit of text that represents a word or a portion of a word. An LLM divides the input into tokens through the tokenizer, then each token is turned into a vector embedding, a numerical representation that the model can understand. During this phase, the LLM takes the entire prompt as input to calculate the key-value (KV) embeddings of each token in each attention layer.

Decoding phase. In the decoding phase, the engine firstly generates a new token based on the prefilled information and then accepts the generated token from the previous step as a single new input token. For each layer, the engine computes the Q, K, V embedding for the new token and performs attention using the new token's Q embedding with all the context's KV-tokens. Unlike prefill phase, generation phase computes only one token in each step.

Memory management of KV cache. Attention mechanisms necessitate the computation of pairwise similarities among all tokens in an input sequence, resulting in a quadratic complexity relative to the sequence length. To mitigate this challenge, KV caching is employed as a compromise between memory

and computational demands. This strategy seeks to prevent the redundant recomputation of key and value tensors for preceding tokens at each generation stage. Instead, these tensors are cached in GPU memory as they are computed throughout the generation process. KV caching is a prevalent optimization technique in the LLM inference process, enabling the compute requirements of the attention mechanism to scale linearly rather than quadratically with the total sequence length.

Initially, LLM serving system statically allocated a significant portion of memory to store KV cache, due to the unpredictable output lengths in LLM inference. This approach, however, resulted in substantial internal and external fragmentation. To mitigate this issue, vLLM introduces PagedAttention, an optimization that enhances memory utilization by segmenting the KV cache into blocks accessed via a lookup table. Through PagedAttention, vLLM facilitates memory sharing not only for the initial prompt blocks but also for other blocks across various requests. Most modern LLM inference frameworks, such as Nvidia’s TensorRT-LLM [42], Huggingface’s TGI [28], adopts ideas similar to PagedAttention.

2.4 Assumptions and Threat Model

In this paper, we explore the deployment of a shared LLM to serve multiple users or applications within a computing system. The employed model is shared among users or applications. Sharing can occur in various scenarios, such as a public LLM service serving multiple users, multiple applications within the same system, or multiple threads within the same application (e.g., browsers). For instance, the same model can be used to provide online chatbot services to multiple users or support local LLM queries for document analysis.

We assume that requests from different users and applications are batched using state-of-the-art techniques for batching and optimization, such as continuous batching and KV caching. Furthermore, we assume that both the attacker’s request and the victim’s request are processed on the same platform, leading to contention and sharing of various caches and optimizations. As a result, this paper aims to investigate whether these optimizations introduce interference and create observable timing side channels.

The attacker only needs to have black-box access to the underlying model, meaning that the model’s architecture and weight parameters remain unknown to the attacker. The attacker is permitted to query the public service or the local model, either in web mode or API mode, and can measure the latency of receiving the response.

We do not consider hardware side channels related to GPU micro-architectures, such as GPU caches [65], residue information leakage [93], or power/frequency side channels [74]. Our primary focus is on software and system-level security aspects. As a result, our attacks possess the capability to target various platforms such as CPU, GPU, and ASIC.

3 Attacks

3.1 Overview

Creating good prompts today is a non-trivial task that requires substantial effort and, in some cases like in-context learning, large amounts of data to achieve the best performance with LLMs. Moreover, prompts may contain sensitive personal information. Thus, prompts are considered valuable resources and should remain private. For example, Samsung Electronics has banned the use of generative AI tools, such as ChatGPT, by employees, due to the leak of confidential data to OpenAI through their use of ChatGPT [2].

This paper considers two types of attacks. The first type involves the recovery of the system prompt, which we call *prompt stealing attacks (PSA)*. The system prompt defines the expected behavior of the model and may contain carefully curated business logic, private information, or safety-related instructions. Thus, an LLM application developer often views its system prompt as intellectual property and keeps it confidential. Having knowledge of the system prompt can also aid in other attacks, such as jailbreaking. The second type of attack is *peeping neighbour attack (PNA)*, which involves recovering the semantics of the initial prompt by other users or applications. Such prompts may contain personally identifiable information (PII) or other sensitive data, and the exposure of user’s prompts may compromise the user’s privacy.

The attack consists of two phases. In the *offline phase*, the attacker learns the timing characteristics related to how a request affects the server’s state and how the state changes will be reflected in the latency of serving a later request. It’s worth noting that the timing characteristics are primarily associated with the optimization techniques rather than a specific model or model parameters. Although the online model is considered unknown to the attacker, the offline phase can be conducted using an attacker-controlled LLM system, utilizing an attacker-controlled model and commonly used optimization techniques.

In the *online phase*, there are three roles involved: the server (S), the victim client (C), and the attacker (A). In the first attack scenario, the attacker aims to infer the prompt from a user or an application. Initially, the server platform operates in state $State_0$. Then C makes a query, the state of the LLM system changes to $State_1$, e.g., certain values are cached in the GPU memory and the priority queues are updated. Since these state changes can impact the performance of subsequent requests, the attacker A immediately (at time frame t_{start}) sends a request r and measures the latency $l = t_{end} - t_{start}$ in order to infer the state changes, where t_{end} is the TTFT of the request. Lastly, the attacker deduces the prompt provided by C by observing these state changes.

In recovering the system prompt, we assume that the attacker can trigger a request both with and without system prompt. We believe the assumption is reasonable, e.g., Ope-

nAI supports both the API mode and web mode, where in the web mode the system automatically concatenates a system prompt for the online chat, while in the API mode, the user chooses the request input freely. To recover the system prompt, the attacker initiates an initial request r_0 . Then the LLM system automatically triggers the state changes caused by the system prompt, using the request $r = r_0 + \text{system_prompt}$. Immediately after that, the attacker \mathcal{A} sends another request r_1 and measures the latency $l = t_{\text{end}} - t_{\text{start}}$ to infer the state changes. Through these state changes, the attacker deduces the content of the *system_prompt*.

3.2 Prompt Stealing Attacks (PSA)

Background. In the process of generating tokens in autoregressive language models such as GPT, all previously generated tokens are fed into the network when a new token is produced. This necessitates the recalculation of the hidden representation for each preceding token with every subsequent generation, resulting in significant computational overhead. KV cache serves as a prevalent optimization method in decoder-only Transformers. It minimizes compute by leveraging the KV cache from the last inference, albeit at the cost of increased memory consumption.

KV cache can also be shared across requests, since many input prompts share text segments (e.g., system messages, prompt templates, and documents provided as context). By precomputing and caching the attention states of these frequently-occurring text segments on the inference server, we can efficiently reuse them when they appear in user prompts. Representative examples of this approach include the automatic prefix sharing in vLLM [58] and Radixattention in SGLang [91].

The side channel. The sharing of KV cache across requests introduces a timing side channel. During the prefill phase, the request will be returned faster if the prefix of the prompt is cached by previous requests since loading key and value tensors from KV cache is much faster than recomputation. Since LLMs usually use stream output (e.g., word by word), we can observe the TTFT at a fine-grained level to detect the timing difference between hit or miss of the KV cache.

Let's estimate the timing difference under a typical LLM deployment setting as an example. Consider a model with 7 billion (Llama-7B) parameters, and an A100 GPU with 312 TFLOPS computation power and 1.5 TB memory bandwidth. In the best case, let us assume the GPU achieves 100% utilization rate. Then if the token misses the cache, the prefilling phase of 1 token takes about:

$$\begin{aligned} \text{prefill time (miss)} &= \# \text{tokens} \times (\# \text{parameters} / \text{GPU compute bandwidth}) \\ &= \frac{1 \text{ token} \times (2 \times 7B) \text{ FLOP/token}}{312 \text{ TFLOP/s}} \\ &\approx 0.045 \text{ ms.} \end{aligned}$$

In comparison, if the token hits the cache, the prefilling phase of 1 token is the time of loading pre-computed KV cache from HBM (assuming 16-bit precision parameters):

$$\begin{aligned} \text{prefill time (hit)} &= \# \text{tokens} \times (\text{KV cache per token} / \text{GPU memory bandwidth}) \\ &= \frac{1 \text{ token} \times (2 \times \# \text{hidden dimension} \times \# \text{layers}) \times 2 \text{ Bytes/token}}{1.5 \text{ TBytes/s}} \\ &= \frac{1 \text{ token} \times (2 \times 4096 \times 32) \times 2 \text{ Bytes/token}}{1.5 \text{ TBytes/s}} \\ &\approx 0.35 \text{ us.} \end{aligned}$$

The timing difference is exacerbated on larger models or when the GPU is servicing concurrent requests. For example, for the Llama-2-70B-Chat-GPTQ (70 billion parameters with 4-bit quantization) model, the prefilling phase of 1 token for missing and hitting the cache is about 0.45 ms and 0.22 us, respectively.

Our proposed prompt stealing attack takes advantage of the timing leakage caused by sharing the KV cache. In particular, an attacker sends a request to the LLM and observes the TTFT to infer (part of) the prompts from concurrent requests to the LLM service. Since the KV cache can only be shared if the prompts share the same prefix, we propose an incremental search algorithm to narrow down the search space token. Our approach is able to recover the prompts on a token-by-token basis. We will describe this algorithm and evaluate it on real systems in Section 4.1 and Section 4.2.

3.3 Peeping Neighbour Attacks (PNA)

Background. Semantic cache (e.g., GPTCache [24, 44]) maintains a cache of previously asked questions and their corresponding responses. It retrieves semantically similar queries from the cache using similarity measures. If a query is found within the similarity threshold, the cached response is returned; otherwise, a new LLM query is made. Semantic caching can significantly improve the cost-effectiveness and performance of LLM, and it is supported by major LLM frameworks such as LangChain [27] and LlamaIndex [29].

The side channel. Reusing semantic cache across multiple users can potentially expose the queries of other users. This is because a cache hit leads to a much faster response than querying the LLM, which creates a noticeable timing difference that can be exploited by attackers. Given that querying the LLM is usually time-consuming, our evaluation shows that the timing difference is typically large, between several milliseconds for hitting the cache and several seconds for missing the cache.

Unlike the KV cache side channel, the reuse of a semantic cache does not necessitate an exact match among prompts. Instead, as long as the caches are semantically similar, they can be reused. This characteristic of the semantic cache side

channel enables an attacker to infer the semantics of concurrent requests from users in close proximity. Consequently, we refer to this type of attack as the peeping neighbour attack.

Considering that the semantic cache is stored locally on disk and can be quite large, it is difficult to clear even with excessive requests. This makes searching for the victim’s target prompt challenging, as the attacker prompts may also be cached and introduce noise. To address these challenges, we propose an efficient search algorithm that minimizes the caching effects from the attacker while maximizing the success rate in detecting the caching of the victim’s prompt. We will present the algorithm and demonstrate how to recover private information embedded in the prompts from a neighboring users in [Section 4.3](#).

4 Evaluation

In this section, we present an empirical evaluation of the characteristics of the discovered side channels, and elaborate on how to exploit them efficiently. To reduce the impact on innocent users of public LLM services, we built the system in the local environment using open-sourced projects, trying to replicate real-world deployment of LLM serving systems.

All our local experiments were conducted on a Lenovo server equipped with an Intel(R) Xeon(R) Silver 4310 CPU (running at 2.10 GHz with 12 cores) and 500 GB of DDR4 memory. The system is equipped with 4 NVIDIA A100 GPUs (each with 40 GB of GPU memory). The system runs on Ubuntu 18.04 OS (kernel version: 5.4.0-150-generic), with GPU driver version 525.125.06, CUDA 11.8, and PyTorch 2.3.1. We used open-source models, including Llama-7B and Llama-2-70B-Chat-GPTQ. Both the server and client were deployed on the same server, communicating through the local loopback network interface.

4.1 Prompt Stealing Attacks (PSA) on System Prompt

Characterizing the leakage. For this evaluation, we used SGLang [40] as a representative system. SGLang reorganizes the KV cache blocks into a radix tree to support efficient prefix matching and KV cache reuse. We conducted experiments to measure the correlation between the token length of matched prefix and the response latency of the model (i.e. TTFT in the single-GPU environment) on llama2-13B and llama2-70B-GPTQ models. We used the public system prompt dataset [6] to generate prompts with different lengths of matched prefix. Besides, we confirmed that the content of the prompt did not result in noticeable differences in the response latency.

To assess the impact of the shared prefix token length on the response latency, in the *first* step, we generated five groups of prompts of the same length as T , and the groups were denoted as T_0, T_1, T_2, T_4 , and T_8 , which shared exactly the

initial k tokens with T for $k = 0, 1, 2, 4$, and 8 , by replacing the k -th token with different tokens in each group. Next, for each prompt within the group, we measured the TTFT when these prompts were fed into the LLM, right after T was fed into the LLM and was cached. In our evaluation we set the group size to 2000, and designated the collected samples from group T_0 (i.e., no shared prefix with T) as 0, and the collected samples from other groups (i.e., shared prefixes of lengths 1, 2, 4, 8 with T) as 1. Finally, we plotted the ROC curves for all datasets to visualize the timing difference in [Figure 1](#). The results clearly demonstrate that as the length of the shared prefix increases, the model exhibits a significant caching effect on TTFT. This effect is more pronounced and stable in larger models.

Building the classifier. In the *offline phase*, we trained a cluster of classifiers, $classifier_0$ to $classifier_{n-1}$, where each $classifier_i$ ($0 \leq i < n$) detects if the i -th token hits the cache, given that all preceding tokens have also hit the cache.

We used the llama2-70B-GPTQ model for evaluation. As shown in [Figure 1](#) (b), the timing difference between a cache hit and miss of 1 token is small (AUC=0.52), making it hard to build a robust classifier. Fortunately, we found that the timing difference can be enlarged by appending one dummy token right after the target token, i.e., adding the dummy token as the $i+1$ -th token when building $classifier_i$. This may be because the dummy token takes up additional GPU computational resources, thus increasing the timing difference.

We now describe the process of generating the dataset used to train $classifier_i$. We first randomly sampled a system prompt P from the dataset. We then generated 2000 unique sentences of length $i+1$ as negative samples, which all have the first $i-1$ tokens in common with P , but differ on the last two tokens. We also generated 2000 unique positive samples, which all have the first i tokens in common with P and a random dummy $(i+1)$ -th token. To collect the latency of the positive and negative samples, we first fed P to the LLM server (SGLang with the llama2-70B-GPTQ model, then sent the sample to the LLM and measured the latency of each sample. Before collecting the latency of next sample, we flushed the KV cache to avoid noises. Based on the collected latency for both positive and negative samples, we utilized the XGBoost algorithm to train the classifier and optimized its hyper parameters using Bayesian optimization. To enhance the performance of the classifier, we adjusted the decision threshold to maximize the difference between the true positive rate (TPR) and false positive rate (FPR), while ensuring that the TPR remains high. In our evaluation, the classifiers have a TPR of 55% and FPR of 42%.

Online attacks to recover the system prompt. To reduce the search space, as shown in [Figure 2](#), in the *online phase*, the targeted prompts are recovered token by token. The process of recovering the next token involves several components: a *next token predictor* that predicts the distribution of the next

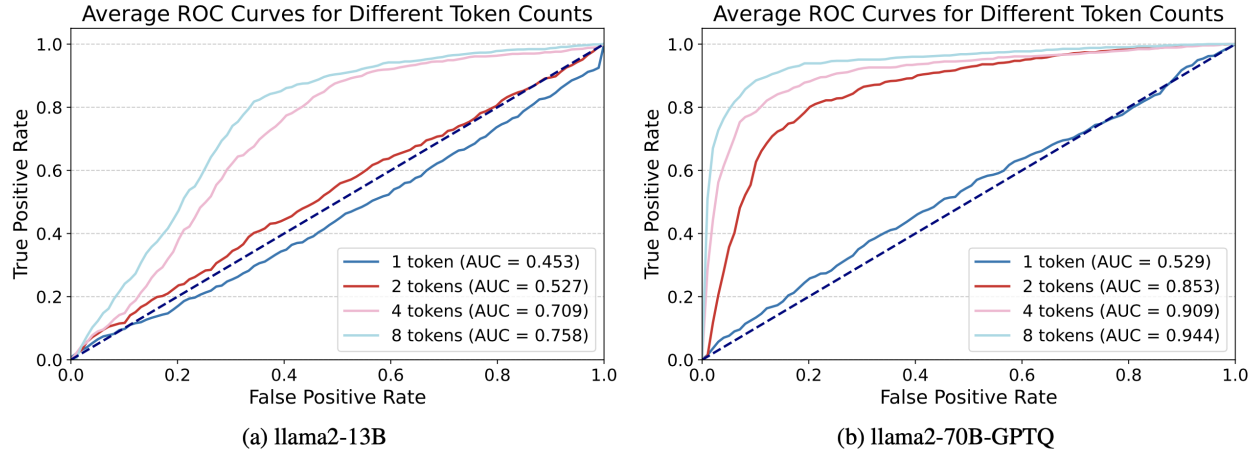


Figure 1: Leakage profile of sharing the KV cache. We used two models with different sizes: llama2-13B and llama2-70B-GPTQ, and plotted the ROC curve to fingerprint the timing difference when the prompts share the prefix of 1, 2, 4 and 8 tokens respectively.

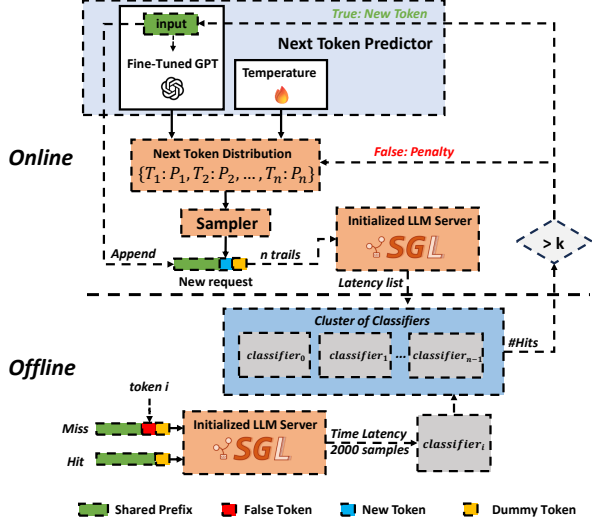


Figure 2: Efficient token-by-token prompt recovery.

token based on the tokens already recovered, a *Sampler* that samples a candidate token according to this predicted distribution. For each candidate of the i -th token, the guessed prompt is fed into the LLM, to produce a set of TTFT values as the input of the $classifier_i$. The pre-trained classifier $classifier_i$ then evaluates the likelihood of the candidate token hitting the cache, indicating whether the token is correct. If it is deemed correct, the token will be appended to the prompt, and we continue to search for the next token. Otherwise, a *repetition penalty* will be returned and applied to the probability corresponding to the current token to adjust the overall probability distribution. Currently, we take a simple way to apply the repetition penalty, by halving the sampling probability of missed tokens in a new round.

For constructing the next token predictor, we assume the attacker has collected a public dataset of the system prompts, and the victim system prompts follow a similar word distribution as the public dataset. Therefore a fine-tuned LLM can be used to predict the next token. For the prediction of the next token, we used *distilgpt2* [3] as the base model, fine-tuned with the *teilmillet/system_prompt* [6] dataset. The model accepts the partially recovered prompt and the temperature as input, subsequently generating a probability distribution for the next token. The incorporation of temperature scaling enables the predictor to have more randomness and diversity in token predictions. Our predictor is far from optimal as we used a single NVIDIA 1080 Ti GPU for fine-tuning, which only took about half an hour. With better fine-tuning settings, e.g. greater batch size, more epochs or a larger language model, the predictor can be further improved.

To improve the classification accuracy, we need to collect a set of TTFT values for the classifier using the same candidate prompts in n repetitive trials. For this purpose, we explicitly flush the cache and begin our timing measurements after the victim prompt is served in the LLM server. To flush the KV cache, we take advantage of SGLang's external APIs, i.e., `sglang.srt.mem_cache.flush_cache` and the web API `http://sglang-server:30000/flush_cache`.¹ We consider the candidate prompt to have hit the cache if the number of hits returned by the classifier exceeds k out of n trials. In our evaluation, we set $n = 100$ and $k = 50$, and the accuracy of correctly identifying a prefix cache hit is more than 86%, and the FPR is about 5%.

We further evaluated our attack on the *teilmil-*

¹Besides explicit API calls, alternative methods could also be used to flush the cache. Specifically, the KV cache in SGLang adopts a simple LRU eviction policy that evicts the least recently used leaf first. Moreover, SGLang evict all cached tokens when the system receives a large batch size of requests. We leave the exploration in this direction as future work.

let/system_prompt [6] dataset, assuming the attacker is familiar with common expressions and vocabulary of system prompts. Specifically, we divided the dataset of 69 samples into 60 for fine-tuning and 9 for the evaluation. With the next token predictor and the classifier above, we can recover the system prompt token by token, achieving an average accuracy of 92.3% in recovering the tokens, with an average of 234 queries to the LLM to recover 1 token.

4.2 Prompt Stealing Attacks (PSA) on RAG

In the current Retrieval-Augmented Generation (RAG) scenario, LLMs generate more specific and accurate responses by knowledge from existing documents or user-uploaded content. In such a scenario, the model will repeatedly use previously accessed documents on one hand, while on the other hand, a small subset of documents will be frequently used in certain specific contexts. Therefore, the KV cache reuse techniques, such as CacheBlend [83] and RAGCache [55] can significantly reduce the response time of the LLM system and increase its throughput. This section presents preliminary findings concerning the KV cache leakage in the RAG scenario.

Inferring the queried document. We conducted our evaluation on the CacheBlend inference framework [30], which is built upon vLLM and supports KV cache reuse. Using the Multi-news dataset [32, 48], we selected documents with different content at various lengths and obtained ROC curves of response times when users queried a specific document, both with and without the document being cached. We selected 500 documents of different lengths and contents from the dataset through simple data processing. When testing the caching effect of documents of different lengths, we first uploaded one of these documents to the LLM. Then, we repeatedly used this document to query the LLM to obtain a dataset of response times for document cache hits. Additionally, we used the remaining documents, which differ from the target document, to query and obtain a dataset of response times for document cache misses. During the AUC calculation, we labeled the response times for document matches as 1 and those for document misses as 0, and plotted the ROC curves for both. The results, as shown in Figure 3, indicate that since document lengths in RAG scenarios are typically in the range of a few hundred words, it becomes apparent whether a document is cached. This could potentially allow for the identification of private documents used by other users.

Inferring the visited website. Side-channel information leakage can occur when users on the same host access browsers and use the same LLM plugin. We examined Lu-mos, an LLM plugin designed to summarize web content and respond to queries. We found that the caching effect occurs when different users access the same web pages and send the same queries, resulting in timing side channels.

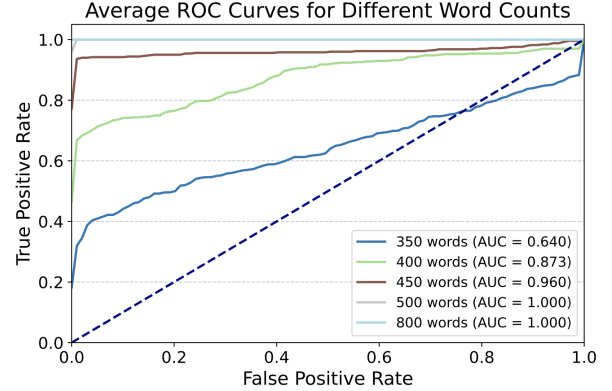


Figure 3: Leakage profile of sharing documents in the RAG scenario, under different document sizes.

Furthermore, we deployed an LLM locally that responds within web pages using Ollama [1], with RedisCache and RedisSemanticCache as the back-end cache. We queried the same prompts with different users in different browsers (e.g., Chrome and Edge) and found that there are significant time differences when the cache is hit, and the response time decreases from several seconds to milliseconds. This further proves the possibility of side-channel attacks.

4.3 Peeping Neighbour Attacks (PNA)

Characterizing the leakage. For this evaluation, we built a local chatbot system based on LangChain framework with GPTCache to cache the requests based on semantic similarity. We used gpt-3.5-turbo in API mode as our backend LLM model and MedQuAD [4] as the dataset. We used ONNX [33] to calculate the semantic similarity between sentences.

As shown in Table 1, we assume a set of public templates that are likely to be used by the users. In reality, users may use different expressions to convey the same meaning as the templates. Meanwhile, users may also include private attributes into the sentences. To characterize the leakage, we would like to measure how the semantic similarity will change with respect to private attributes (e.g. name, medical condition etc.). More specifically, we would like to investigate whether the semantic differences introduced from the private attributes are significant enough to be recognized, given that users can freely choose the expressions with the same semantics as the templates.

The evaluation steps are shown in Figure 4. We took a specific template “Compose a meeting agenda ... for [Name] with [medical condition].”, denoted by T_0 as an example. In this case, both name and medical condition are private attributes of the patient. In the *first* step, we randomly sampled 10 names from the python package NameDataset. To obtain 10 random medical conditions, we randomly sampled 10 se-

Table 1: Examples of user prompts that contain private attributes.

Use cases	Prompts
Healthcare	Compose a meeting agenda for an interdisciplinary team discussing the treatment plan for [Name] with [medical condition].
Travel planning	I'm [flying/driving] to [destination] with [Name] for a leisurely trip, and we'll be staying at [hotel] for [number of days]. Can you create a comprehensive packing list organized by category?
Business planning	Act as an expert business plan writer, and help me generate a product and services section of my [business type] business plan. My company is [business] called [business name] that specializes in [USP or specialization].
Performance review	I'm preparing for the annual performance review of an employee named [Name]. [Name]'s role involves [roles]. Draft a performance review for [Name] and suggesting improvements in [area of improvement].
E-mails	Draft an e-mail to the [company] on [subject].
Cover letter	Write a conversational cover letter for [Name] for a job application as a [position] at [company].
Out-of-office message	Write a short out-of-office message. Reason: [vacation]. Dates: [month and dates]. Person to contact in an emergency or for immediate help: [name] at [email address].

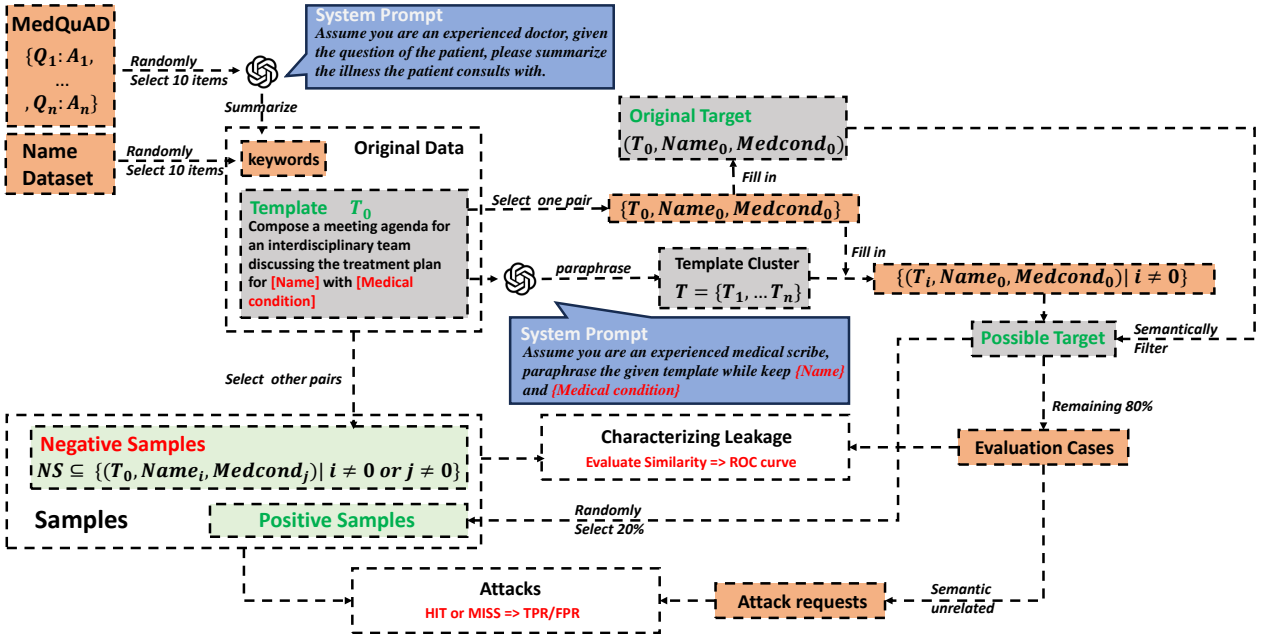


Figure 4: Peeping neighbour attacks.

mantically unrelated Q&A pairs from MedQuAD dataset and used gpt-3.5-turbo to summarize the medical conditions from questions. We randomly sampled 1 name and 1 medical condition, denoted by $Name_0$ and $Medcond_0$, as the private attributes to be recovered, while the other pairs are used to generate negative group (described in the next paragraph).

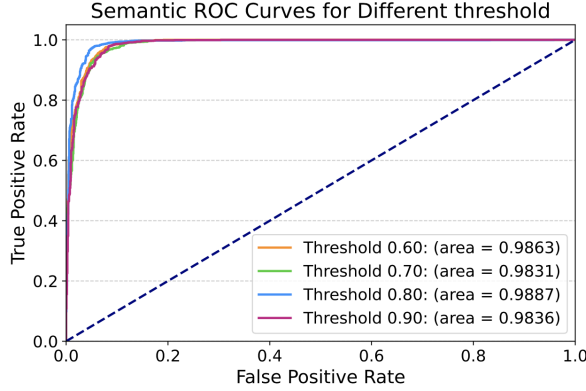
In the *second* step, we aimed to generate a set of expressions with similar meaning as the template T_0 . For this purpose, we paraphrased the template (T_0) using gpt-3.5-turbo and generated n semantically similar sentences $\{T_1, \dots, T_n\}$ with $Name_0$ and $Medcond_0$ filled in the template. In this step, irrelevant templates were filtered out if their semantic similarity with T_0 is below a predefined threshold (we used the same value as GPTCache's default threshold).

After the above two steps, we've generated two groups

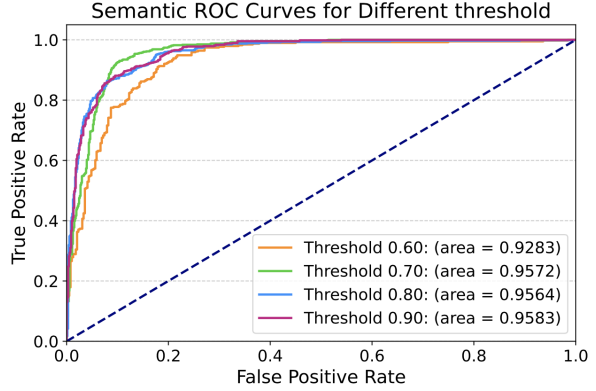
of samples: the positive group consists of all generated templates filled with $Name_0$ and $Medcond_0$, i.e., $\{(T_i, Name_0, Medcond_0) | i = 1, \dots, n\}$; the negative set consists of the original template filled with other names and medical conditions, i.e., $\{(T_0, Name_j, Medcond_j) | i \neq 0 \text{ or } j \neq 0\}$. Moreover, we splitted the positive group into two subsets: the first one (20%) is used as positive samples, and the rest are used as evaluation cases. We made sure the positive group and negative group are of the same size.

In the last step, we computed the semantic similarity between the evaluation cases and the positive group, as well as between the evaluation cases and the negative group. This process yields the respective similarity vectors of the positive and negative groups.

We evaluated the semantic differences under different se



(a) The “name” and “medical condition” in the negative group are both different from the positive group.



(b) Either the “name” or “medical condition” in the negative group is different from the positive group.

Figure 5: Leakage profile of sharing the semantic cache. We plotted the ROC curve to fingerprint the timing difference between the similarity vectors of the positive and negative groups.

mantic thresholds ranged from 0.6 to 0.9 (the default value in GPTCache is 0.8), and the ROC curves between the similarity vectors of the positive and negative groups are shown in Figure 5 (a). It can be seen that the positive and negative group can be well distinguished. For example, in the default setting (threshold = 0.8), when the TPR is close to 0.95, the FPR is still less than 0.1.

Besides, we further evaluated the effect of the cases when only 1 private attribute matches. For this purpose, the negative group consists of sentences with only one correct private attribute using the same template, while the positive group remains unchanged. The result (Figure 5 (b)) shows that the semantic differences between the positive group and negative group are still large enough. For example, in the default setting (threshold = 0.8), when the TPR is close to 0.85, the FPR is still less than 0.1.

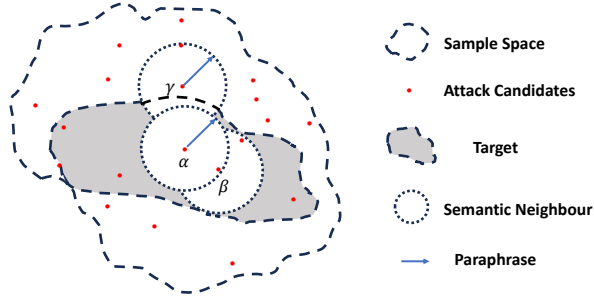


Figure 6: The greedy searching algorithm for PNA.

Attacks. The ROC curves in Figure 5 show the accuracy of inferring the private attribute. To improve the attack accuracy, there are two main strategies for selecting attack prompts: selecting the requests that are *most representative* of the attack

space; and increasing the number of attack attempts.

We define the *most representative* requests as those that are nearest to other requests in the sentence space with the same semantics. Specifically, we use *distilbert-base-uncased* as the model to obtain the embeddings of all sentences in the sentence space and employ euclidean normalization methods to sort the requests by L2 distances from low to high. Therefore, the smaller the index of a sentence within the group, the more representative it is for the entire sentence space. After sorting, we can use sentences with smaller indexes as attack prompts to increase the coverage of the attack.

Moreover, the attacker can also improve attack coverage by issuing more attack prompts. Given the low FPR, if any of these prompts hit the cache, the attacker can infer a semantic cache hit. Since these prompts can also be cached and may add noise to the semantic cache, it is important for the attacker to select sentences that will not be considered similar (i.e., orthogonal prompts) as attack prompts. Notably, adding more attack prompts increases the FPR even if the coverage increases.

As shown in Figure 6, we designed a greedy searching algorithm that aims to find the *most representative* requests for a target sentence. Specifically, suppose that the target space (a subspace of the whole space, denoted by shaded area) is the sentences that are judged as semantically similar with the target sentence, then the attack goal is to expand the coverage within the target space by sending orthogonal prompts. For this purpose, in every searching step, we always select the one in the sentence space that is most representative in the remaining candidate set (e.g., α) and add it into the attack set. If the most representative one (e.g., β) is too close to any member of the attack set, we skip it and continue to search for the next one. The process stops if any of the following conditions is met: there are no remaining candidates in the

sentence space, or the FPR exceeds a preset number σ .

In the evaluation, both the positive and negative groups contained 695 sentences. We set the threshold σ to 0.04, and identified 4 orthogonal attack prompts with the proposed greedy search algorithm. [Table 2](#) shows the TPR and FPR when the number of attack prompts increases from 1 to 4. In particular, the attack can achieve a 85.3% TPR and 3.2% FPR with only 1 trial, while the attack can achieve a 96.2% TPR and 3.9% FPR with 4 trials.

Table 2: Attack accuracy with different number of attack trials.

#Trials	TPR (%)	FPR (%)
1	85.3	3.2
2	91.9	3.3
3	95.1	3.6
4	96.2	3.9

4.4 Measurement Study

KV cache sharing. To investigate potential caching mechanisms in LLM services, we conducted the experiments on multiple LLMs by invoking the APIs provided by these vendors. These APIs support different roles, including system, user, and assistant etc. We designed requests with system and user prompts of varying lengths and configured them in streaming mode.

We created two user accounts for each LLM service. First, we measured the response latency of the initial chunk in the streaming reply from the first account. Then, we repeated the process with the second account, sending identical requests multiple times. By comparing the latency of the first request with subsequent ones, we identified lower latencies in later requests, indicating the use of caching mechanisms in the LLM services. We conducted continuous tests in the same time period as much as possible to increase the likelihood of co-locating on the same physical machine and the prompts are cached. To verify that the latency reduction is due to KV cache sharing, we set the temperature to 0.9 and checked if the LLM generated different responses. If it did, this indicated that KV cache sharing was supported, which can reduce the TTFT while still allowing for diverse responses. To minimize network latency effects, we sent requests using system prompts of varying lengths (from 200 to about 2,000 tokens). The time difference between cached and uncached responses is usually several hundred milliseconds, making it easy to distinguish. Moreover, it can be observed that when the cache is hit, TFTT is independent of the system prompt's length, whereas when the cache is missed, TFTT significantly increases with the system prompt's length.

To evaluate the document sharing support, we used the LLM APIs to load both identical and different documents of

various sizes (see [Section 4.2](#)). We then queried each document with the same question: "Please summarize the document." We considered an LLM service to support document sharing if subsequent requests exhibited lower latencies than the first request. As summarized in [Table 3](#), most popular LLM service providers support KV cache sharing in certain scenarios.

Table 3: Summary of KV cache sharing in real world LLM serving systems (date: 08/29/2024).

LLM service	System prompt sharing	User prompt sharing	Document sharing
GPT-4-turbo (OpenAI)	✓	✓	✗
Claude-3.5	✓	✓	✗
Qwen-max	✗	✗	✗
Moonshot [68]	✓	✓	✓
Ernie-8k (Baidu) [18]	✗	✗	✗
Gemini (Google) [20]	✗	✗	✓
Fireworks.ai [19]	✓	✓	✗
Groq [25]	✗	✗	✗
SiliconFLow [41]	✓	✓	✗

Table 4: Native support of semantic caching of popular AI service providers (date: 08/29/2024).

Service providers	Semantic cache support
Azure OpenAI Service models [22]	✓
Amazon Bedrock [11]	✓
Google Vertex AI [43]	✗
Alibaba Elastic Algorithm Service (EAS) of Platform for AI (PAI) [10]	✓

Semantic cache sharing. Firstly, we manually reviewed the documentation of public cloud AI service providers to confirm whether they support semantic cache APIs. As shown in [Table 4](#), semantic caching can significantly reduce the cost of LLM services and is supported by major AI platform-as-a-service providers. Notably, even on platforms that do not offer native semantic caching, users may still employ their own or open-source solutions, such as GPTCache.

We also investigated whether popular chatbots support semantic caching. To evaluate a target chatbot, we used the customized questions listed in [Table 1](#) and queried the chatbot multiple times with the same question, recording their responses and latency. If the latency was lower than the first query and the responses were identical, this strongly indi-

Table 5: Summary of semantic caching in real world LLM serving systems (date: 08/29/2024).

Chatbot	Semantic cache
ChatGPT [13]	✗
Google Gemini chat [21]	✓
Claude chat [15]	✗
Yi-Chat [7]	✓
iFLYTEK Spark chat [8]	✓
Qwen chat [38]	✗
Kimi chat [26]	✗
Deepseek chat [16]	✓
OSS Chat [34]	✓
Canonical Chat [39]	✓
Twig [9]	✓

cated the presence of semantic caching, leading us to mark the chatbot as supporting it. As shown in Table 5, we observed semantic caching in many popular online chatbots.

5 Mitigations

In this section, we provide preliminary results on mitigating the attacks discussed in the paper.

5.1 Mitigating KV Cache Leaks

Design. A straightforward approach to mitigate KV cache leakages is to remove any sharing across requests, but this would invalidate all computation and cost savings. We note that the prompt stealing attack recovers the prompt token by token by observing the per-token timing difference. In this section, we study the effect of a simple mitigation strategy where the prefix cache can only be shared in units of at least K tokens ($K = 2, 3, 4$ etc.). In SGLang, this could be achieved by modifying the radix tree structure for managing the KV cache. Besides, the scheduling policy in SGLang can be modified to only prioritize prompts with a minimum number of K shared prefix tokens, and prompts with less than K shared prefix tokens should still be placed in the waiting list. This approach reduces the likelihood of KV cache sharing, but is unlikely to have a significant impact on performance.

Evaluation. To evaluate the effectiveness of the mitigation, we conducted a simulation-based experiment that used an *oracle* to emulate the actual LLM queries, thereby reducing the time required to query the LLM. For each value of K ($K = 1, 2, 3, 4$), we selected a threshold that maximizes the difference between TPR and FPR while preserving a high TPR. The oracle then simulated the classifier by randomly sampling a number and determining whether it falls within the classification range.

Table 6: Token recovery results under different numbers of minimum shared tokens.

K	Recovery rate	Accuracy	#Queries/token
1	100%	92.8%	229.7
2	98.6%	100%	117.1
3	87.0%	96.7%	176.7
4	68.1%	100%	348.1

In the evaluation, we used the same repetitive trails method, dataset and fine-tuned model as in Section 4.1. Since the timing difference is more prominent when increasing K , we reduced the number of queries (i.e., n) to the oracle while still maintaining a high classification accuracy. Table 6 presents the recovery rate of tokens and the average number of queries to recover 1 token for $K = 1, 2, 3$ and 4. The result shows that even with a larger K , the attack can still achieve good performance. However, since the search space increases significantly when increasing K , the attack requires more guesses and more queries to the LLM. It is interesting to see that increasing K from 1 to 2 even makes the attack more efficient (with higher accuracy and fewer queries), since the timing difference between matching 0 or 2 tokens are more pronounced than when $K = 1$, and we can recover every token with fewer false negatives and queries.

5.2 Mitigating Semantic Cache Leaks

Design. As investigated in Section 4.3, private information significantly influences the semantic similarity between sentences. Consequently, the peeping neighbor attack infers this private information by probing whether a semantically similar request is cached within the system. To counteract this attack, we proposed a mitigation strategy that involved the identification and anonymization of privacy information present in user inputs. This approach not only eliminates the leakage of private information but also enhances the potential for sharing requests among users.

As shown in Figure 7, we integrated a custom pre-processor and post-processor into the GPTCache framework. The pre-processor was designed to identify private data within the input text, and replace sensitive information with their anonymized identifiers. In our mitigation, we de-identified PII attributes selectively, including names, email addresses, phone numbers, credit card numbers, and IP addresses, so as not to remove any information that is necessary for LLMs.

To facilitate reuse, the Data Manager defines a mapping structure that stores the anonymized text alongside its corresponding plain counterpart in a key-value format. Subsequently, the post-processor identifies the anonymized identifiers within the response and substitutes them with their real counterparts by referencing the mapping structure. This en-

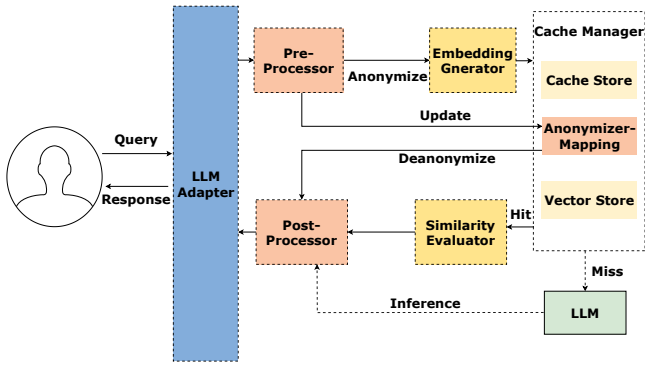


Figure 7: Defense on the privacy leakage of semantic similarity sentences

sures that the user receives a response that is both precise and adheres to privacy regulations.

Evaluation. In our prototyped implementation, we employed the Presidio [5] tool designed by Microsoft to automatically identify private attributes. To measure the overhead, we used the evaluation dataset released by Presidio, which contained sentences with private information. We randomly sampled 1000 data from the dataset and fed them into the original GPT-Cache and anonymized GPTCache respectively, and calculated the average time of the pre-processor and post-processor. The average delay caused by anonymization is about 6 ms, while the time for GPTCache to process a semantic-cache-hit request without anonymization is approximately 0.14 s. Therefore, de-identification introduces only about 4% additional performance overhead, which does not affect the overall performance of GPTCache significantly.

6 Discussions

Unexplored timing leakages. This paper utilizes SGLang [40] and GPTCache [24] as the most representative KV cache and semantic cache sharing mechanisms. However, it is important to note that more sophisticated optimization techniques may enhance performance, but they could also amplify the significance of timing leakage. For example, modular prefix caching [50] and CacheBlend [83] facilitate KV caching for not only prefix tokens but also intermediate ones. Cascade inference [85] stores the shared KV cache in GPU shared memory (SMEM for short), for fast access in multiple requests. The sharing of KV cache in speculative decoding [59] may also introduce speculative side channels, akin to Spectre [56]. Besides, this paper only considers shared public LLM services. Sharing KV caches may also occur on local deployed LLMs with the trend of LLM as an OS [63]. We leave the further exploration of the impact of the discovered side channels to future work.

Co-locations. Co-location is a prerequisite for timing side-channel attacks. There has been significant research on how to achieve co-location in the cloud for micro-architectural side channels [71, 75, 89, 92]. Co-location can be more efficient on LLM platforms since existing LLM systems focus on improving cache reuse through optimized scheduling policies. For example, since the baseline scheduling policy, such as first-come-first-serve, is not aware of the shared prompt within each LLM platform, requests are intermingled across all LLM engines, precluding the reuse of the common prompt prefix and potentially resulting in suboptimal cache reuse. To address this issue, LLM serving systems like SGLang [40], Parrot [60] and Mooncake [68] have introduced modified schedulers that prioritize requests that align with cached prefixes, a strategy referred to as cache-aware scheduling.

7 Related Works

Prompt extraction attacks with adversarial prompts. Most existing works focus on stealing system or prompts from LLMs by making LLMs print the previous prompts, through directly printing and translation, etc. For example, a twitter user has claimed to discover the prompt used by Bing Chat [17]. Earlier works construct the attacker prompt manually [67, 88], while a recent work called PLeak takes advantage of the output feedback for a given input prompt and proposes an incremental search algorithm to optimize the search of the prompt [54]. Zhang et al. present a framework for systematically measuring the effectiveness of these attacks. These works exploit the model’s susceptibility to adversarial prompts, while our proposed attacks exploit the timing differences introduced in LLM service deployment; therefore, our attacks do not depend on details of specific LLMs.

Side channel attacks on LLM. Debenedetti et al. propose system-level side channels, within component in the deep learning lifecycle, including training data filtering, input pre-processing, output monitoring, and query filtering. These can potentially be exploited to infer either the training data or test queries [46]. In comparison, we exploit the timing leakage caused by the optimization in system deployment of LLM inference rather than the output to recover the input prompt.

LLM keystroking attacks [79] are a type of side channel analysis that is based on package analysis. These attacks reveal the length of the response token, contingent upon the assumption that the attacker has access to encrypted network packets. Since this type of attack relies on the length of tokens being inferred from the packet, it can be mitigated by obscuring token size.

Micro-architectural side channel attacks on deep learning systems. Numerous studies have been conducted to extract deep learning models or structures, or fingerprinting deep learning models, by exploiting CPU side channels [47, 52, 69, 72, 82], GPU side channels [77], FPGA side

channel [87], power and magnetic side channels [53, 62], PCIe traffic [95] etc. Our work diverges from these studies in that we aim to leak the private prompts, rather than stealing the model parameters. Furthermore, our approach does not depend on micro-architectural or power characteristics of specific hardware but relies on timing leakages inherent in LLM systems. Consequently, our attacks can be executed on CPU, GPU, and FPGA platforms as long as they employ KV cache or semantic cache sharing techniques.

8 Conclusions

Inference in LLMs is a resource-intensive process, leading to numerous studies on methods to reduce inference costs and latency. These optimization techniques often involve various caches and speculative decoding strategies. However, when multiple users and applications share a platform, these optimizations can cause interference among different users. This paper investigates the side channels resulting from such interference, identifying two types of leakages: one in the KV cache and another in the semantic cache. We urge LLM system researchers to recognize this new threat and prioritize security in their designs.

Ethical Considerations & Disclosure

We follow standard best practices to ensure that our study follows ethical principles [57]. The evaluations were performed in a controlled local environment. All targeted system prompts or user prompts are collected from public data without any personal information. In the black-box measurement of online LLM services, we only send prompts and receive responses. In this process, we only infer whether our own requests are cached by observing the response latency. We do not intend to recover the system prompt or private prompt with the discovered side channel for these online services. As this study is based on publicly available data and does not involve any human participants, it is not considered as human subjects research by our Institutional Review Boards (IRB).

While publishing our results can raise concerns about misuse, we believe that raising awareness of the problem is even more important, as it can inform LLM vendors and the research community to build more robust systems. We have reported our findings to all the developers (SGLang, GPT-Cache etc.), and LLM service providers (OpenAI, Claude and Google Gemini etc.) as soon as we identified the side channels. Our reports were delivered via the official security report portal or by separate e-mails. As of the preparation of this manuscript, they were still investigating this issue, and we remain in communication with them.

Open Science

We will make all the code and datasets required to reproduce our experiments publicly available after the paper is published.

References

- [1] Ollama. <https://ollama.com/download>.
- [2] Samsung bans staff’s ai use after spotting chatgpt data leak. <https://www.bloomberg.com/news/articles/2023-05-02/samsung-bans-chatgpt-and-other-generative-ai-use-by-staff-after-leak>.
- [3] Distilgpt2. <https://huggingface.co/distilbert/distilgpt2>, 2019.
- [4] Medquad. <https://huggingface.co/datasets/lavita/MedQuAD>, 2019.
- [5] Presidio. <https://github.com/microsoft/presidio>, 2022.
- [6] System prompt. https://huggingface.co/datasets/teilmillet/system_prompt, 2023.
- [7] 01.ai api platform. <https://platform.lingyiwanwu.com/chat>, 2024.
- [8] 01.ai api platform. <https://xinghuo.xfyun.cn/desk>, 2024.
- [9] Ai brain for ex. <https://www.twig.so/>, 2024.
- [10] Alibaba platform for ai. <https://www.alibabacloud.com/help/en/pai/>, 2024.
- [11] Amazon bedrock - build generative ai applications with foundation models. <https://aws.amazon.com/bedrock/>, 2024.
- [12] Bingchat. <https://www.bing.com/chat>, 2024.
- [13] Chatgpt. <https://chatgpt.com>, 2024.
- [14] Chatgpt | openai. <https://openai.com/chatgpt/>, 2024.
- [15] Claude. <https://claude.ai/>, 2024.
- [16] Deepseek. <https://chat.deepseek.com/>, 2024.
- [17] The entire prompt of microsoft bing chat. <https://twitter.com/kliu128/status/1623472922374574080>, 2024.
- [18] Ernie. <https://wenxin.baidu.com/>, 2024.

[19] Fireworkai. <https://fireworks.ai/models>, 2024.

[20] Gemini. <https://deepmind.google/technologies/gemini/>, 2024.

[21] Gemini. <https://gemini.google.com/app>, 2024.

[22] Get cached responses of azure openai api requests. <https://learn.microsoft.com/en-us/azure/api-management/azure-openai-semantic-cache-lookup-policy>, 2024.

[23] Github copilot · your ai pair programmer. <https://github.com/features/copilot/>, 2024.

[24] Gptcache : A library for creating semantic cache for llm queries. <https://github.com/zilliztech/gptcache>, 2024.

[25] Groq. <https://groq.com/>, 2024.

[26] Kimi chat. <https://qianwen.aliyun.com/>, 2024.

[27] Langchain. <https://www.langchain.com/>, 2024.

[28] Large language model text generation inference. <https://github.com/huggingface/text-generation-inference>, 2024.

[29] Llmaindex is a data framework for your llm applications. https://github.com/run-llama/llama_index, 2024.

[30] Llm inference with cacheblend. <https://github.com/YaoJiayi/CacheBlend>, 2024.

[31] Lumos. <https://github.com/andrewnguonly/Lumos>, 2024.

[32] Multi-news. <https://github.com/Alex-Fabbri/Multi-News>, 2024.

[33] Onnx. <https://github.com/onnx/onnx>, 2024.

[34] Osschat: Chat with open source software. <https://osschat.io/>, 2024.

[35] Perplexity ai. <https://www.perplexity.ai/>, 2024.

[36] Prompt caching with claude. <https://www.anthropic.com/news/prompt-caching>, 2024.

[37] Prompt template. https://python.langchain.com/docs/modules/model_io/prompts/prompt_templates/, 2024.

[38] Qwen 2.5. <https://qianwen.aliyun.com/>, 2024.

[39] Semantic cache by canonical ai. <https://canonical.chat/>, 2024.

[40] Sqlang is yet another fast serving framework for large language models and vision language models. <https://github.com/sql-project/sqlang>, 2024.

[41] Siliconflow. <https://siliconflow.cn/>, 2024.

[42] Tensorrt-llm. <https://github.com/NVIDIA/TensorRT-LLM>, 2024.

[43] Vertex ai with gemini 1.5 pro and gemini 1.5 flash. <https://cloud.google.com/vertex-ai>, 2024.

[44] Fu Bang. Gptcache: An open-source semantic cache for llm applications enabling faster answers and cost savings. In *Proceedings of the 3rd Workshop for Natural Language Processing Open Source Software (NLP-OSS 2023)*, pages 212–218, 2023.

[45] Tri Dao, Dan Fu, Stefano Ermon, Atri Rudra, and Christopher Ré. Flashattention: Fast and memory-efficient exact attention with io-awareness. *Advances in Neural Information Processing Systems*, 35:16344–16359, 2022.

[46] Edoardo Debenedetti, Giorgio Severi, Nicholas Carlini, Christopher A Choquette-Choo, Matthew Jagielski, Milad Nasr, Eric Wallace, and Florian Tramèr. Privacy side channels in machine learning systems. In *33rd USENIX Security Symposium*, 2024.

[47] Vasisht Duddu, Debasis Samanta, D Vijay Rao, and Valentina E Balas. Stealing neural networks via timing side channels. *arXiv preprint arXiv:1812.11720*, 2018.

[48] Alexander R. Fabbri, Irene Li, Tianwei She, Suyi Li, and Dragomir R. Radev. Multi-news: A large-scale multi-document summarization dataset and abstractive hierarchical model. In *Annual Meeting of the Association for Computational Linguistics*, 2019.

[49] Elias Frantar, Saleh Ashkboos, Torsten Hoefer, and Dan Alistarh. Gptq: Accurate post-training quantization for generative pre-trained transformers. *arXiv preprint arXiv:2210.17323*, 2022.

[50] In Gim, Guojun Chen, Seung-seob Lee, Nikhil Sarda, Anurag Khandelwal, and Lin Zhong. Prompt cache: Modular attention reuse for low-latency inference. *Proceedings of Machine Learning and Systems*, 6:325–338, 2024.

[51] Louie Giray. Prompt engineering with chatgpt: a guide for academic writers. *Annals of biomedical engineering*, 51(12):2629–2633, 2023.

[52] Cheng Gongye, Yunsi Fei, and Thomas Wahl. Reverse-engineering deep neural networks using floating-point timing side-channels. In *2020 57th ACM/IEEE Design Automation Conference (DAC)*, pages 1–6. IEEE, 2020.

[53] Peter Horvath, Lukasz Chmielewski, Leo Weissbart, Lejla Batina, and Yuval Yarom. Barracuda: Bringing electromagnetic side channel into play to steal the weights of neural networks from nvidia gpus. *arXiv preprint arXiv:2312.07783*, 2023.

[54] Bo Hui, Haolin Yuan, Neil Gong, Philippe Burlina, and Yinzhi Cao. Pleak: Prompt leaking attacks against large language model applications. *arXiv preprint arXiv:2405.06823*, 2024.

[55] Chao Jin, Zili Zhang, Xuanlin Jiang, Fangyue Liu, Xin Liu, Xuanzhe Liu, and Xin Jin. Ragcache: Efficient knowledge caching for retrieval-augmented generation. *arXiv preprint arXiv:2404.12457*, 2024.

[56] Paul Kocher, Jann Horn, Anders Fogh, Daniel Genkin, Daniel Gruss, Werner Haas, Mike Hamburg, Moritz Lipp, Stefan Mangard, Thomas Prescher, et al. Spectre attacks: Exploiting speculative execution. *Communications of the ACM*, 63(7):93–101, 2020.

[57] Tadayoshi Kohno, Yasemin Acar, and Wulf Loh. Ethical frameworks and computer security trolley problems: Foundations for conversations. In *32nd USENIX Security Symposium (USENIX Security 23)*, pages 5145–5162, 2023.

[58] Woosuk Kwon, Zhuohan Li, Siyuan Zhuang, Ying Sheng, Lianmin Zheng, Cody Hao Yu, Joseph Gonzalez, Hao Zhang, and Ion Stoica. Efficient memory management for large language model serving with page-dattention. In *Proceedings of the 29th Symposium on Operating Systems Principles (SOSP)*, pages 611–626, 2023.

[59] Yaniv Leviathan, Matan Kalman, and Yossi Matias. Fast inference from transformers via speculative decoding. In *International Conference on Machine Learning*, pages 19274–19286. PMLR, 2023.

[60] Chaofan Lin, Zhenhua Han, Chengruidong Zhang, Yuqing Yang, Fan Yang, Chen Chen, and Lili Qiu. Parrot: Efficient serving of llm-based applications with semantic variable. *arXiv preprint arXiv:2405.19888*, 2024.

[61] Zechun Liu, Barlas Oguz, Changsheng Zhao, Ernie Chang, Pierre Stock, Yashar Mehdad, Yangyang Shi, Raghuraman Krishnamoorthi, and Vikas Chandra. Llm-qat: Data-free quantization aware training for large language models. *arXiv preprint arXiv:2305.17888*, 2023.

[62] Henrique Teles Maia, Chang Xiao, Dingzeyu Li, Eitan Grinspun, and Changxi Zheng. Can one hear the shape of a neural network?: Snooping the gpu via magnetic side channel. In *USENIX Security Symposium*, pages 4383–4400, 2022.

[63] Kai Mei, Zelong Li, Shuyuan Xu, Ruosong Ye, Yingqiang Ge, and Yongfeng Zhang. Aios: Llm agent operating system. *arXiv e-prints*, pages arXiv–2403, 2024.

[64] Xupeng Miao, Gabriele Oliaro, Zhihao Zhang, Xinhao Cheng, Hongyi Jin, Tianqi Chen, and Zhihao Jia. Towards efficient generative large language model serving: A survey from algorithms to systems. *arXiv preprint arXiv:2312.15234*, 2023.

[65] Hoda Naghibijouybari, Ajaya Neupane, Zhiyun Qian, and Nael Abu-Ghazaleh. Rendered insecure: Gpu side channel attacks are practical. In *Proceedings of the 2018 ACM SIGSAC conference on computer and communications security*, pages 2139–2153, 2018.

[66] Seungcheol Park, Jaehyeon Choi, Sojin Lee, and U Kang. A comprehensive survey of compression algorithms for language models. *arXiv preprint arXiv:2401.15347*, 2024.

[67] Fábio Perez and Ian Ribeiro. Ignore previous prompt: Attack techniques for language models. *arXiv preprint arXiv:2211.09527*, 2022.

[68] Ruoyu Qin, Zheming Li, Weiran He, Mingxing Zhang, Yongwei Wu, Weimin Zheng, and Xinran Xu. Mooncake: Kimi’s kvcache-centric architecture for llm serving. *arXiv preprint arXiv:2407.00079*, 2024.

[69] Adnan Siraj Rakin, Md Hafizul Islam Chowdhury, Fan Yao, and Deliang Fan. Deepsteal: Advanced model extractions leveraging efficient weight stealing in memories. In *2022 IEEE symposium on security and privacy (SP)*, pages 1157–1174. IEEE, 2022.

[70] Laria Reynolds and Kyle McDonell. Prompt programming for large language models: Beyond the few-shot paradigm. In *Extended abstracts of the 2021 CHI conference on human factors in computing systems*, pages 1–7, 2021.

[71] Thomas Ristenpart, Eran Tromer, Hovav Shacham, and Stefan Savage. Hey, you, get off of my cloud: exploring information leakage in third-party compute clouds. In *Proceedings of the 16th ACM conference on Computer and communications security*, pages 199–212, 2009.

[72] Shubhi Shukla, Manaar Alam, Pabitra Mitra, and Debdip Mukhopadhyay. Stealing the invisible: Unveiling pre-trained cnn models through adversarial examples and timing side-channels. *arXiv preprint arXiv:2402.11953*, 2024.

[73] Yixin Song, Zeyu Mi, Haotong Xie, and Haibo Chen. Powerinfer: Fast large language model serving with a consumer-grade gpu. *arXiv preprint arXiv:2312.12456*, 2023.

[74] Hritvik Taneja, Jason Kim, Jie Jeff Xu, Stephan Van Schaik, Daniel Genkin, and Yuval Yarom. Hot pixels: Frequency, power, and temperature attacks on {GPUs} and arm {SoCs}. In *32nd USENIX Security Symposium (USENIX Security 23)*, pages 6275–6292, 2023.

[75] Venkatanathan Varadarajan, Yingqian Zhang, Thomas Ristenpart, and Michael Swift. A placement vulnerability study in Multi-Tenant public clouds. In *24th USENIX Security Symposium (USENIX Security 15)*, pages 913–928, 2015.

[76] Wenxiao Wang, Wei Chen, Yicong Luo, Yongliu Long, Zhengkai Lin, Liye Zhang, Binbin Lin, Deng Cai, and Xiaofei He. Model compression and efficient inference for large language models: A survey. *arXiv preprint arXiv:2402.09748*, 2024.

[77] Junyi Wei, Yicheng Zhang, Zhe Zhou, Zhou Li, and Mohammad Abdullah Al Faruque. Leaky dnn: Stealing deep-learning model secret with gpu context-switching side-channel. In *2020 50th Annual IEEE/IFIP International Conference on Dependable Systems and Networks (DSN)*, pages 125–137. IEEE, 2020.

[78] Xiuying Wei, Yunchen Zhang, Xiangguo Zhang, Ruihao Gong, Shanghang Zhang, Qi Zhang, Fengwei Yu, and Xianglong Liu. Outlier suppression: Pushing the limit of low-bit transformer language models. *Advances in Neural Information Processing Systems*, 35:17402–17414, 2022.

[79] Roy Weiss, Daniel Ayzenshteyn, Guy Amit, and Yisroel Mirsky. What was your prompt? a remote keylogging attack on ai assistants. *arXiv preprint arXiv:2403.09751*, 2024.

[80] Guangxuan Xiao, Ji Lin, Mickael Seznec, Hao Wu, Julien Demouth, and Song Han. Smoothquant: Accurate and efficient post-training quantization for large language models. In *International Conference on Machine Learning*, pages 38087–38099. PMLR, 2023.

[81] Guangxuan Xiao, Yuandong Tian, Beidi Chen, Song Han, and Mike Lewis. Efficient streaming language models with attention sinks. *arXiv preprint arXiv:2309.17453*, 2023.

[82] Mengjia Yan, Christopher W Fletcher, and Josep Torrellas. Cache telepathy: Leveraging shared resource attacks to learn {DNN} architectures. In *29th USENIX Security Symposium (USENIX Security 20)*, pages 2003–2020, 2020.

[83] Jiayi Yao, Hanchen Li, Yuhang Liu, Siddhant Ray, Yihua Cheng, Qizheng Zhang, Kuntai Du, Shan Lu, and Junchen Jiang. Cacheblend: Fast large language model serving with cached knowledge fusion. *arXiv preprint arXiv:2405.16444*, 2024.

[84] Zhewei Yao, Reza Yazdani Aminabadi, Minjia Zhang, Xiaoxia Wu, Conglong Li, and Yuxiong He. Zeroquant: Efficient and affordable post-training quantization for large-scale transformers. *Advances in Neural Information Processing Systems*, 35:27168–27183, 2022.

[85] Zihao Ye, Ruihang Lai, Bo-Ru Lu, Chien-Yu Lin, Size Zheng, Lequn Chen, Tianqi Chen, and Luis Ceze. Cascade inference: Memory bandwidth efficient shared prefix batch decoding, February 2024.

[86] Gyeong-In Yu, Joo Seong Jeong, Geon-Woo Kim, Soo-jeong Kim, and Byung-Gon Chun. Orca: A distributed serving system for Transformer-Based generative models. In *16th USENIX Symposium on Operating Systems Design and Implementation (OSDI 22)*, pages 521–538, 2022.

[87] Yicheng Zhang, Rozhin Yasaei, Hao Chen, Zhou Li, and Mohammad Abdullah Al Faruque. Stealing neural network structure through remote fpga side-channel analysis. *IEEE Transactions on Information Forensics and Security*, 16:4377–4388, 2021.

[88] Yiming Zhang and Daphne Ippolito. Prompts should not be seen as secrets: Systematically measuring prompt extraction attack success. *arXiv preprint arXiv:2307.06865*, 2023.

[89] Yingqian Zhang, Ari Juels, Michael K Reiter, and Thomas Ristenpart. Cross-tenant side-channel attacks in paas clouds. In *Proceedings of the 2014 ACM SIGSAC Conference on Computer and Communications Security*, pages 990–1003, 2014.

[90] Youpeng Zhao, Di Wu, and Jun Wang. Alisa: Accelerating large language model inference via sparsity-aware kv caching. *arXiv preprint arXiv:2403.17312*, 2024.

[91] Lianmin Zheng, Liangsheng Yin, Zhiqiang Xie, Jeff Huang, Chuyue Sun, Cody Hao Yu, Shiyi Cao, Christos Kozyrakis, Ion Stoica, Joseph E Gonzalez, et al. Efficiently programming large language models using sclang. *arXiv preprint arXiv:2312.07104*, 2023.

[92] Wu Zhenyu, Xu Zhang, and H Wang. Whispers in the hyper-space: high-speed covert channel attacks in the cloud. In *USENIX Security symposium*, pages 159–173, 2012.

- [93] Zhe Zhou, Wenrui Diao, Xiangyu Liu, Zhou Li, Kehuan Zhang, and Rui Liu. Vulnerable gpu memory management: towards recovering raw data from gpu. *arXiv preprint arXiv:1605.06610*, 2016.
- [94] Xunyu Zhu, Jian Li, Yong Liu, Can Ma, and Weiping Wang. A survey on model compression for large language models. *arXiv preprint arXiv:2308.07633*, 2023.
- [95] Yuankun Zhu, Yueqiang Cheng, Husheng Zhou, and Yantao Lu. Hermes attack: Steal {DNN} models with lossless inference accuracy. In *30th USENIX Security Symposium (USENIX Security 21)*, 2021.